AGU PUBLICATIONS

Geophysical Research Letters

RESEARCH LETTER

10.1002/2014GL062850

Key Points:
- Glider-based observations were made of the influence of an iceberg
- Submesoscale meltwater patches require high-resolution observations
- The iceberg meltwater stimulates biological productivity

Supporting Information:
- Figure S1

Correspondence to:
L. C. Biddle,
louise.biddle@uea.ac.uk

Citation:
Biddle, L. C., J. Kaiser, K. J. Heywood, A. F. Thompson, and A. Jenkins (2015), Ocean glider observations of iceberg-enhanced biological production in the northwestern Weddell Sea, *Geophys. Res. Lett.*, *42*, 459–465, doi:10.1002/2014GL062850.

Received 11 DEC 2014
Accepted 20 DEC 2014
Accepted article online 28 DEC 2014
Published online 27 JAN 2015

Ocean glider observations of iceberg-enhanced biological production in the northwestern Weddell Sea

Louise C. Biddle[1], Jan Kaiser[1], Karen J. Heywood[1], Andrew F. Thompson[2], and Adrian Jenkins[3]

[1]Centre for Ocean and Atmospheric Sciences, School of Environmental Sciences, University of East Anglia, Norwich, UK, [2]California Institute of Technology, Pasadena, California, US, [3]British Antarctic Survey, Cambridge, UK

Abstract Icebergs affect local biological production around Antarctica. We used an ocean glider to observe the effects of a large iceberg that was advected by the Antarctic Slope Current along the continental slope in the northwestern Weddell Sea in early 2012. The high-resolution glider data reveal a pronounced effect of the iceberg on ocean properties, with oxygen concentrations of (13 ± 4) μmol kg^{-1} higher than levels in surrounding waters, which are most likely due to positive net community production. This response was confined to three areas of water in the direct vicinity of the iceberg track, each no larger than 2 km^2. Our findings suggest that icebergs have an impact on Antarctic production presumably through local micronutrient injections, on a scale smaller than typical satellite observations of biological production in the Southern Ocean.

1. Introduction

Almost half of the mass loss from Antarctica is attributed to iceberg calving [*Depoorter et al.*, 2013]. Atmospheric warming increases iceberg production from the Antarctic Peninsula into the Weddell Sea [*Scambos et al.*, 2000]. Icebergs enhance primary productivity [*Martin et al.*, 1990; *Raiswell et al.*, 2008; *Lancelot et al.*, 2009] and recent studies have described icebergs as "Lagrangian estuaries"; a localized nutrient and iron (Fe) rich environment that encourages phytoplankton blooms [*Smith et al.*, 2007, 2011]. Additional melting ice may therefore have a significant impact on the ecosystem of the Antarctic coastal seas. Ocean color remote sensing, using 10 years of data, showed that the effect of icebergs on production varied between October and March, depending on the existing environmental conditions [*Schwarz and Schodlok*, 2009]. For example, on average during February, an iceberg caused a decrease in chlorophyll *a* concentrations, thought to be due to an increase in vertical mixing, resulting in dilution of the surface phytoplankton concentration. There are in situ observations of delivery of Fe by icebergs with the potential to enhance productivity [*Martin et al.*, 1990; *Raiswell et al.*, 2008; *Lancelot et al.*, 2009; *Smith et al.*, 2007], but these observations are inconsistent with the apparent decrease in chlorophyll *a* concentrations observed by *Schwarz and Schodlok* [2009]. One of the methods of mixing proposed by *Schwarz and Schodlok* [2009] to enhance productivity (or dilute chlorophyll *a*) is caused by basal and sidewall melting of the iceberg. The meltwater is fresher than ambient waters and so relatively buoyant [*Huppert and Turner*, 1980; *Jenkins*, 1999]. This upwelling promotes turbulent mixing through the water column. Depending on the conditions, the upwelled water may enhance phytoplankton growth through micronutrient injection into the surface layer or dilute chlorophyll *a* concentrations [*Neshyba*, 1977; *Sancetta*, 1992; *Vernet et al.*, 2011]. Mechanical mixing can also occur at the keel depth of the iceberg, where the movement of the ice stirs up waters and sediment nearby. Besides injecting micronutrients through enhanced mixing, icebergs carry terrigenous materials that are released during melting, providing another source of particulate iron [*Raiswell et al.*, 2008; *Lancelot et al.*, 2009; *Shaw et al.*, 2011]. In the Weddell Sea, icebergs and low-salinity surface waters were found to be enriched in dissolved iron [*Lin et al.*, 2011].

The northwestern Weddell Sea, where the Antarctic Slope Current carries icebergs along the continental slope around the Powell Basin, is known as "iceberg alley" [*Thompson and Heywood*, 2008; *Gladstone et al.*, 2001; *Stuart and Long*, 2011]. While the population of icebergs in this area is relatively dense, the scarcity of in situ observations of iceberg-related biological activity is in part due to the logistics of accessing this remote region and also the ship time required to identify and track a suitable iceberg for study. A glider deployment there surveyed biological, chemical, and physical properties at high-spatial and high-temporal

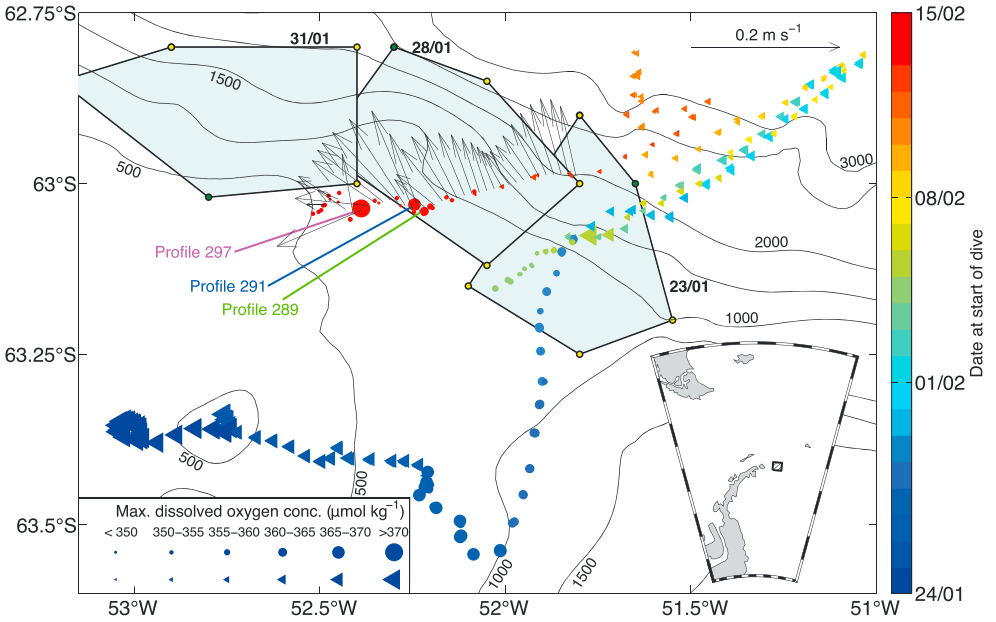

Figure 1. Maximum dissolved oxygen concentration shown by size of symbol (see legend), measured during each vertical profile completed by the glider (two profiles per dive, see Figure S1 in the supporting information), with bathymetry contours every 500 m. Circles represent profiles in or near the Antarctic Slope Current (ASC), and triangles are the remaining profiles from the mission. The iceberg outlines are from Polarview synthetic aperture radar satellite imagery, with one corner colored green to highlight the spinning of the iceberg. The three profiles of interest (289, 291, and 297) can be seen near the outline of the iceberg on 28/01. Arrows indicate the dive-averaged current measured from the glider and show the strong currents that indicate the ASC.

resolutions close to a large iceberg. Here we present evidence of enhanced biological production in surface waters affected by the iceberg and describe how small-scale patchiness is an underestimated feature of Southern Ocean production.

2. Data Collection

As part of the GENTOO (Gliders: Exciting New Tools for Observing the Ocean) project, Seaglider SG522, Beluga, [*Eriksen et al.*, 2001] surveyed the continental shelf and slope in the northwestern Weddell Sea between January and March 2012 (Figure 1). The Seaglider is an autonomous underwater vehicle that profiles between the surface and 1000 m on a dive slope of approximately 25°, giving an effective spacing between full depth dives of approximately 4 km (see Figure S1 in the supporting information). During 310 profiles, the glider, equipped with a Seabird CT sail, Aanderaa oxygen optode, and a WETLabs ECO Triplet, measured pressure, temperature, salinity, dissolved oxygen concentration, chlorophyll and CDOM (Colored Dissolved Organic Matter) fluorescence, and optical backscatter (532 nm).

The TEOS-10 absolute salinity (S_A) [*IOC et al.*, 2010] and conservative temperature (Θ) scales are used to report all salinity and temperature values. Outliers and surface spikes were identified and removed from the glider salinity and dissolved oxygen data. Salinity was calibrated against in situ water samples collected during deployment. Dissolved oxygen concentrations could not be calibrated against Winkler titrations but are of the expected magnitude when adjusted for the colder Antarctic temperatures (within 20 µmol kg^{-1} of air saturation at the surface). However, this is not a problem, as the method used here to calculate net community production [*Riser and Johnson*, 2008] only requires measurement of a change in oxygen concentration over time. Chlorophyll *a* and CDOM concentrations were derived from the fluorescence measurements using the manufacturer's calibration curves.

Synthetic Aperture Radar (SAR) satellite data were obtained from Polar View Antarctica (www.polarview.aq) to track a large iceberg (C-19c, 39 km × 22 km) that transited through the northwest Weddell Sea during the cruise, between 23 and 31 January (Figure 1). It traveled cyclonically along the continental shelf break, west of the Powell Basin (Figure 1). Satellite ocean color observations were not available during the study

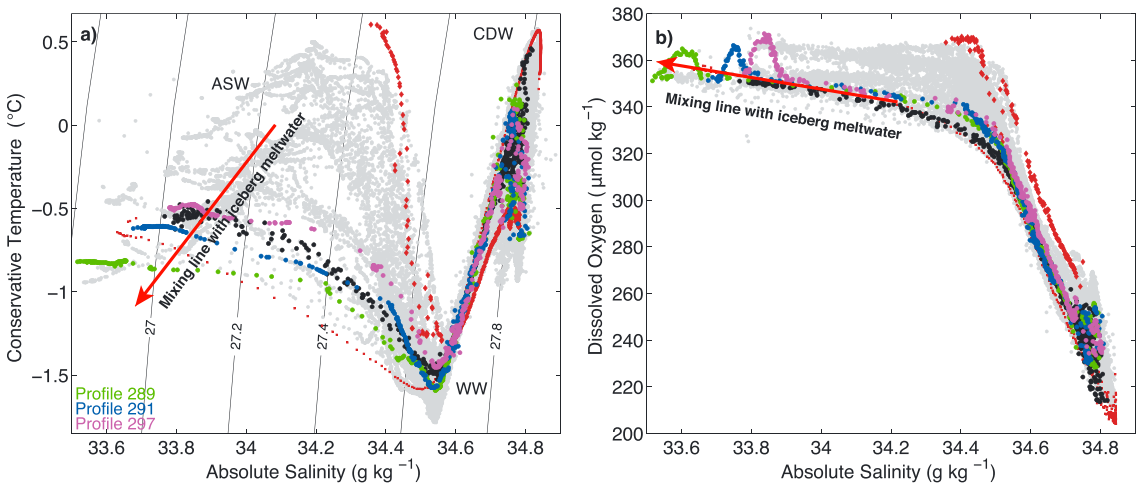

Figure 2. Glider data showing the three main water masses; Antarctic Surface Water (ASW), Winter Water (WW), and Circumpolar Deep Water (CDW), where any data points lying between these water masses indicate mixing between them. (a) Conservative temperature against absolute salinity; (b) dissolved oxygen against salinity. It also highlights the three profiles of interest (289, 291, and 297, in color); grey profiles represent other profiles in the ASC (selected through the hydrographic definition of the ASC), and the brown lines represent the other two groups of profiles (dots are in deeper waters, squares are on shelf). The black lines represent profiles 283–310. The red arrows represent the mixing line between surface waters and iceberg meltwater.

period, as clouds obscured the area of interest. *Schwarz and Schodlok* [2009] and *Arrigo et al.* [2008] also encountered this problem during the same season (late summer).

The Antarctic Slope Front is located using a hydrographic definition; the shoreward extent of the 0°C isotherm and an oxygen minimum concentration of >240 µmol kg^{-1} occur at a neutral density anomaly of 28.2 [*Jacobs*, 1991; *Thompson and Heywood*, 2008]. We define glider profiles lying within, and immediately on the flanks of, the Antarctic Slope Front as those with minimum dissolved oxygen concentrations between 235 and 245 µmol kg^{-1} at a potential density anomaly of 27.8. These profiles are shown in Figure 1, where the glider's depth-averaged current vectors also show the Antarctic Slope Current.

3. Results and Discussion

Three main water masses are identified in the glider data by their hydrographic characteristics (Figure 2a): relatively warm and saline Circumpolar Deep Water (34.8 g kg^{-1}; CDW), the temperature minimum layer (Winter Water, WW), and the relatively fresh (33.4 g kg^{-1}—from sea ice melt over summer) Antarctic Surface Water, cooling toward the freezing point (−1.83°C) as autumn proceeds. Dissolved oxygen concentrations decrease from around the air saturation value of 370 µmol kg^{-1} to 200 µmol kg^{-1} for CDW (Figure 2b).

Three glider profiles (289, 291, and 297), close to the shelf break at isobaths of 600–800 m, show the signature of iceberg meltwater in the top 15 m (Figure 3). These three profiles are each no farther than 2 km from other profiles that do not show the same features, suggesting a representative scale of this meltwater signature. The profiles have cooler and fresher surface water than those nearby (profiles 283–310; on average by 0.1°C and 0.1 g kg^{-1} lower; Figures 3a and 3b) and show mixing between WW and a cold, fresh water mass in their Θ-S_A profiles (Figure 2a). There is no peak in the chlorophyll fluorescence measured on these profiles (Figure 3d), but CDOM concentration and optical backscatter have peaks at depths shallower than 5 m. These profiles exhibit the highest values of these latter parameters of the entire deployment of the glider at 7.93 µg L^{-1} and 0.0323 m^{-1} sr^{-1} (Figures 3e and 3f). These CDOM and backscatter peaks indicate high levels of yellow-brown particles in the water, which can represent dead algae or terrigenous material deposited by the iceberg [*Raiswell et al.*, 2008; *Lin et al.*, 2011].

These profiles are also distinguishable by their higher dissolved oxygen concentrations compared with other profiles above similar isobaths (Figure 1). They show striking peaks in dissolved oxygen concentrations at 8–12 m depth (average 9 µmol kg^{-1} higher than average local values; Figures 2b and 3c). The depth of the dissolved oxygen concentration enhancement in profile 297 is much greater than those in profiles 289 and 291 (Figure 3c). Other than the latter two profiles that show a decrease, it shows increased temperature and salinity compared to surrounding waters, which is likely due to its location on the inshore side of the ASC

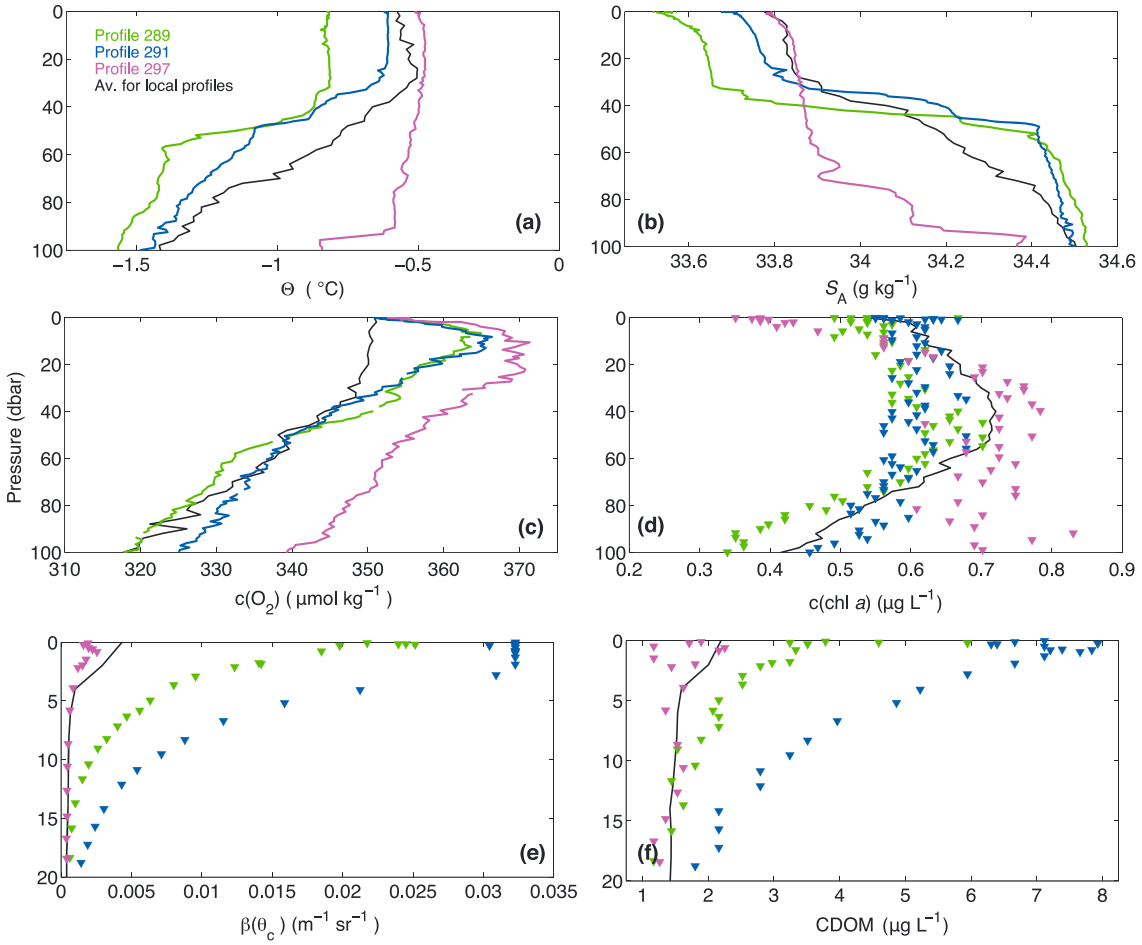

Figure 3. Glider profiles of (a) conservative temperature, (b) absolute salinity, (c) dissolved oxygen concentration, (d) chlorophyll *a* fluorescence, (e) backscatter, and (f) colored dissolved organic matter (CDOM). The colored lines or triangles represent data collected on the profiles of interest, while the black lines represent the average values from profiles surrounding the area of interest (profiles 283–310).

(Figure 1).The elevated dissolved oxygen concentrations could be due to glacial meltwater: the dissolved oxygen concentration in pure (zero salinity) iceberg meltwater is calculated to be (1120 ± 95) µmol kg^{-1} [*Hellmer et al.*, 1998; *Martinerie et al.*, 1992]. Assuming this value, we can calculate the meltwater contribution to measured oxygen concentrations for each glider profile.

$$S_a A + S_{MW}(1 - A) = S_O, \tag{1}$$

$$A = \frac{S_O}{S_a}. \tag{2}$$

$$c(O_{2,a})A + c(O_{2,MW})(1 - A) = c(O_{2,b}). \tag{3}$$

This calculation is shown in equations (1)–(3), where the salinity observed (S_O), the meltwater salinity (S_{MW}), and the average salinity (S_a, from local profiles) are used to calculate the fraction of meltwater present, $(1 - A)$. This value is used to calculate how much oxygen is added to the average oxygen concentration ($c(O_{2,a})$) by the meltwater ($c(O_{2,MW})$), resulting in $c(O_{2,b})$. This is represented in Figure 2b, where the uncertainty relating to the pure meltwater oxygen value is not shown, as the change in slope of the line is indistinguishable at these salinities. The measured values for the average profiles can be seen to follow this mixing line in Figure 2b, but the three profiles that observed the striking peaks show values greater than that expected from meltwater-dissolved oxygen alone.

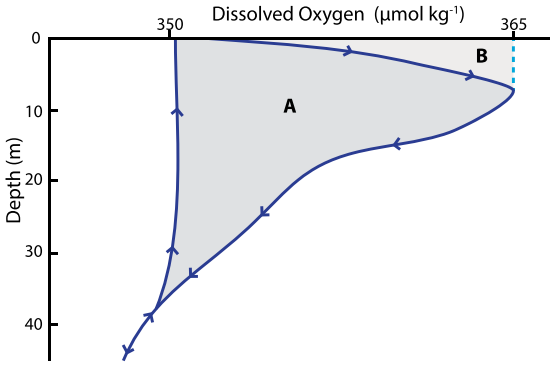

Figure 4. Schematic from profile 291 illustrating how the additional oxygen was calculated. The difference between profile 291 and average dissolved oxygen concentration from the local area (area A) provides the excess dissolved oxygen inventory. Since the meltwater influence likely extended to the surface, area B is added to area A in the NCP calculation to correct for any oxygen lost due to air-sea exchange [following *Riser and Johnson*, 2008].

Icebergs can deposit micronutrients (including dissolved iron) through meltwater, which can enhance biological production [*Raiswell et al.*, 2008; *Lin et al.*, 2011], which in turn increases dissolved oxygen concentrations. The combination of the evidence for meltwater and a mechanism for enhanced biological production of oxygen from icebergs shows that these dissolved oxygen concentration peaks were caused by iceberg-enhanced biological production. The production is most likely stimulated by iceberg micronutrients deposited at the surface, as opposed to nutrient-rich CDW being upwelled. Upwelled CDW would show distinct warmer, saltier anomalies in the Θ-S_A profiles, but the meltwater appears here as colder, fresher, and only within the top 15 m. There are also four profiles between 289 and 299 that do not show any influence from the iceberg (profiles 293–296). Figure 1 shows that these profiles are in the core of the Antarctic Slope Current, indicating that any micronutrients or possible signs of production would have been advected away quickly.

The iceberg passed through the area of observed meltwater between 27 and 29 January, while the glider sampled the water on 14 February. *Schwarz and Schodlok* [2009] found that SeaWiFS ocean color data showed peak production rates 6 days after an iceberg's passage, while in situ observations still recorded elevated chlorophyll *a* concentrations up to 10 days after [*Helly et al.*, 2011]. This may explain why no peak in chlorophyll fluorescence is observed 17 days after the iceberg's passage, as the glider has sampled waters after the biological production peak, when chlorophyll *a* concentrations have returned to background values.

An estimate of the Net Community Production (NCP) can be made from the amount of additional dissolved oxygen observed in the profiles affected by iceberg meltwater. As the dissolved oxygen measurements are not calibrated against in situ water samples, the difference between the dissolved oxygen concentrations in profile 289 or 291 and the background dissolved oxygen concentrations is used to represent the oxygen added through production, similar to methods used by *Riser and Johnson* [2008]. The dissolved oxygen concentrations calculated in equation (3) ($c(O_{2,b})$) include $c(O_{2,MW})$ and so are used as the background values.

The dissolved oxygen concentration is integrated between the points where the elevated O_2 profile intersects the background O_2 profile (shown in Figure 3). The difference between these profiles corresponds to an increase in the dissolved oxygen inventory of (328 ± 9) mmol m^{-2} between 0 and 37.5 m for profile 291 (Figure 4). We assume that this increase is entirely due to NCP over (16 ± 2) days. This requires an NCP of (21 ± 3) mmol m^{-2} d^{-1} O_2 to produce the dissolved oxygen observed. A correction can be made for air-sea gas exchange by assuming that the peak-dissolved oxygen concentration was initially present at the surface (dotted line, Figure 4, following *Riser and Johnson* [2008]). Integrating along the new line and following the same methodology as before results in an O_2 inventory increase of (422 ± 9) mmol m^{-2}, corresponding to an NCP of (27 ± 4) mmol m^{-2} d^{-1} O_2. Using the approximation that NCP(O_2) divided by the photosynthetic quotient is equal to net primary production (14C-NPP; [*Marra*, 2009]), 14C-NPP is calculated to be (232 ± 34) mg m^{-2} d^{-1}. This is comparable to values found by *Vernet et al.* [2011] in the Weddell Sea (average of (275.7 ± 123.1) mg m^{-2} d^{-1}). The same method was used for profiles 289 and 297, which resulted in 14C-NPP values of (77 ± 14) mg m^{-2} d^{-1} and (615 ± 82) mg m^{-2} d^{-1}, respectively.

Enhanced biological production caused by micronutrients from an iceberg has been reported before [*Martin et al.*, 1990; *Raiswell et al.*, 2008; *Lancelot et al.*, 2009], but what is important about these glider observations

is the spatial scale and timing of the production. The production is affected by fine-scale variability in the region, with productive profiles less than 2 km from profiles showing no enhanced production. This small-scale patchiness of the production would not be visible on typical MODIS or SeaWiFS chlorophyll products, with a resolution of 4 or 9 km (e.g., those used by *Arrigo et al.*, [2008]). However, the satellite imagery is available in up to 1 km resolution [e.g., *Schwarz and Schodlok*, 2009], which is likely to resolve these features, and the use of which should be encouraged. Yet *Schwarz and Schodlok* [2009] did not identify any similar small-scale production features and also observed lower chlorophyll *a* concentrations in February around icebergs. A further complication is the high levels of cloud cover around Antarctica. At about 60°S, the annual mean cloud cover is 65–70% [*King and Turner*, 1997], which during the "growing" season of October to March could correspond to 118 days of cloud cover. Neither MODIS or SeaWiFS imagery was available for the period covered by this study, suggesting that cloud cover could cause significant underestimates in local production rates.

The lack of any evidence for an increase in chlorophyll *a* in the profiles affected by meltwater and increased production may suggest that there is a decoupling between chlorophyll *a* concentrations and carbon removal and that NCP may be enhanced even where there is no observable chlorophyll *a* increase. This decoupling could be due to the time lag between the production and observations being made resulting in accumulation of the dissolved oxygen. Alternatively, the community structure of phytoplankton could lead to variations in the carbon to chlorophyll *a* ratio [*Westberry and Behrenfeld*, 2014]. This can explain why no increase was seen in chlorophyll *a* concentrations around icebergs [*Schwarz and Schodlok*, 2009]. The cause of decoupling is potentially an important mechanism that requires further study.

4. Conclusion

Ocean gliders deployed in the northwestern Weddell Sea observed lower temperature and salinity and increased dissolved oxygen, CDOM and backscatter at depths between 5 and 15 m following the passage of a large iceberg. The dissolved oxygen concentrations were higher than values expected from iceberg meltwater, indicating that biological production had occurred, most likely due to the deposition of micronutrients from the iceberg. There was no observed enhancement of chlorophyll *a* concentrations, suggesting a decoupling between NCP and chlorophyll *a* concentrations. This is a mechanism that will require a focused study in the future.

All properties showed submesoscale spatial variability. On such small scales, even sampling by gliders have limitations; out of over 80 profiles in the direct track of the iceberg, only three showed a signature of biological production. These smaller, localized production zones are an important consideration for future calculations of Southern Ocean production. Previous reports have suggested that icebergs have little, or no, effect on biological production in the later summer months [*Schwarz and Schodlok*, 2009]. More high-resolution observations are required to identify how frequent these localized production areas are in order to quantify more accurately their overall effect on the Southern Ocean carbon budget. Ocean gliders may prove to be an invaluable resource for iceberg studies, as they have the potential to move in closer to the waters surrounding an iceberg than a ship can.

Acknowledgments

The GENTOO project and glider deployments were supported by NERC Antarctic Funding Initiative grant NE/H01439X/1. L.C.B. was supported by a NERC PhD studentship at UEA. We thank ship crew, officers, and scientific party of cruise JR255 on board RRS *James Clark Ross*. The data for this paper are available from the British Oceanographic Data Centre. We thank Robert Raiswell and John Helly for constructive comments on an earlier version of this paper.

The Editor thanks Rob Raiswell and John Helly for their assistance in evaluating this paper.

References

Arrigo, K. R., G. L. van Dijken, and S. Bushinsky (2008), Primary production in the Southern Ocean, 1997–2006, *J. Geophys. Res.*, *113*, C08004, doi:10.1029/2007JC004551.

Depoorter, M. A., J. L. Bamber, J. A. Griggs, J. T. M. Lenaerts, S. R. M. Ligtenberg, M. R. van den Broeke, and G. Moholdt (2013), Calving fluxes and basal melt rates of Antarctic ice shelves, *Nature*, *502*(7469), 89–92.

Eriksen, C., T. Osse, R. Light, T. Wen, T. Lehman, P. Sabin, J. Ballard, and a. M. Chiodi (2001), Seaglider: A long-range autonomous underwater vehicle for oceanographic research, *IEEE J. Oceanic Eng.*, *26*(4), 424–436, doi:10.1109/48.972073.

Gladstone, R., G. Bigg, and K. Nicholls (2001), Iceberg trajectory modeling and meltwater injection in the Southern Ocean, *J. Geophys. Res.*, *106*(19), 903–15.

Hellmer, H., S. S. Jacobs, and A. Jenkins (1998), Oceanic erosion of a floating Antarctic glacier in the Amundsen Sea, in *Ocean, Ice, and Atmosphere: Interactions at the Antarctic Continental Margin*, edited by H. Hellmer, S. S. Jacobs, and A. Jenkins, pp. 83–99, AGU, Washington, D. C.

Helly, J. J., R. S. Kaufmann, G. R. Stephenson, and M. Vernet (2011), Cooling, dilution and mixing of ocean water by free-drifting icebergs in the Weddell Sea, *Deep Sea Res., Part II*, *58*(11-12), 1346–1363, doi:10.1016/j.dsr2.2010.11.010.

Huppert, H. E., and J. S. Turner (1980), Ice blocks melting into a salinity gradient, *J. Fluid Mech.*, *100*(2), 367–384.

IOC, SCOR, and IAPSO (2010), The international thermodynamic equation of seawater 2010: Calculation and use of thermodynamics properties, in *Intergovernmental Oceanographic Commission, Manuals and Guides 56*, p. 196, UNESCO, Paris.

Jacobs, S. S. (1991), On the nature and significance of the Antarctic Slope Front, *Mar. Chem.*, *35*(1-4), 9–24, doi:10.1016/S0304-4203(09)90005-6.

Jenkins, A. (1999), The impact of melting ice on ocean waters, *J. Phys. Oceanogr.*, *3*, 2370–2381.
King, J. C., and J. Turner (1997), *Antarctic Meteorology and Climatology*, Cambridge Univ. Press.
Lancelot, C., A. de Montety, H. Goosse, S. Becquecvort, V. Schoemann, B. Pasquer, and M. Vancoppenolle (2009), Spatial distribution of the iron supply to phytoplankton in the Southern Ocean: A model study, *Biogeosciences*, *6*, 2861–2878.
Lin, H., S. Rauschenberg, C. R. Hexel, T. J. Shaw, and B. S. Twining (2011), Free-drifting icebergs as sources of iron to the Weddell Sea, *Deep Sea Res., Part II*, *58*(11-12), 1392–1406, doi:10.1016/j.dsr2.2010.11.020.
Marra, J. (2009), Net and gross productivity: Weighing in with 14C, *Aquat. Microb. Ecol.*, *56*, 123–131, doi:10.3354/ame01306.
Martin, J., R. Gordon, and S. Fitzwater (1990), Iron in Antarctic waters, *Nature*, *345*, 156–158.
Martinerie, P., D. Raynaud, D. M. Etheridge, J.-M. Barnola, and D. Mazaudier (1992), Physical and climatic parameters which influence the air content in polar ice, *Earth Planet. Sci. Lett.*, *112*(1-4), 1–13, doi:10.1016/0012-821X(92)90002-D.
Neshyba, S. (1977), Upwelling by icebergs, *Nature*, *267*, 507–508.
Raiswell, R., L. Benning, M. Tranter, and S. Tulaczyk (2008), Bioavailable iron in the Southern Ocean: The significance of the iceberg conveyor belt, *Geochem. Trans.*, *9*, 7, doi:10.1186/1467-4866-9-7.
Riser, S. C., and K. S. Johnson (2008), Net production of oxygen in the subtropical ocean, *Nature*, *451*(7176), 323–325.
Sancetta, C. (1992), Primary production in the glacial North Atlantic and North Pacific oceans, *Nature*, *360*, 249–251.
Scambos, T., C. Hulbe, M. Fahnestock, and J. Bohlander (2000), The link between climate warming and break-up of ice shelves in the Antarctic Peninsula, *J. Glaciol.*, *46*, 516–530.
Schwarz, J. N., and M. P. Schodlok (2009), Impact of drifting icebergs on surface phytoplankton biomass in the Southern Ocean: Ocean colour remote sensing and in situ iceberg tracking, *Deep Sea Res., Part I*, *56*, 1727–1741, doi:10.1016/j.dsr.2009.05.003.
Shaw, T., R. Raiswell, C. Hexel, H. Vu, W. Moore, R. Dudgeon, and K. L. Smith Jr. (2011), Input, composition, and potential impact of terrigenous material from free-drifting icebergs in the Weddell Sea, *Deep Sea Res., Part II*, *58*(11-12), 1376–1383, doi:10.1016/j.dsr2.2010.11.012.
Smith, K., A. Sherman, T. Shaw, and J. Sprintall (2011), Icebergs as unique Lagrangian ecosystems in polar seas, *Annu. Rev. Mar. Sci.*, *5*(1), 269-287.
Smith, K. L., B. H. Robison, J. J. Helly, R. S. Kaufmann, H. A. Ruhl, T. J. Shaw, B. S. Twining, and M. Vernet (2007), Free-drifting icebergs: Hot spots of chemical and biological enrichment in the Weddell Sea, *Science*, *317*, 478–482, doi:10.1126/science.1142834.
Stuart, K., and D. Long (2011), Tracking large tabular icebergs using the SeaWinds Ku-Band microwave scatterometer, *Deep Sea Res., Part II*, *58*, 1285–300.
Thompson, A. F., and K. J. Heywood (2008), Frontal structure and transport in the northwestern Weddell Sea, *Deep Sea Res., Part I*, *55*, 1229–1251, doi:10.1016/j.dsr.2008.06.001.
Vernet, M., K. Sines, D. Chakos, A. O. Cefarelli, and L. Ekern (2011), Impacts on phytoplankton dynamics by free-drifting icebergs in the NW Weddell Sea, *Deep Sea Res., Part II*, *58*(11-12), 1422–1435, doi:10.1016/j.dsr2.2010.11.022.
Westberry, T. K., and M. J. Behrenfeld (2014), Oceanic net primary production, in *Biophysical Applications of Satellite Remote Sensing*, edited by J. M. Hanes, pp. 205–230, Springer, Berlin, Germany.